Orbital angular momentum of entangled counterpropagating photons

Juan P. Torres, Clara I. Osorio, and Lluis Torner

ICFO—Institut de Ciencies Fotoniques, and Department of Signal Theory and Communications, Universitat Politecnica de Catalunya, 08034 Barcelona, Spain

Received March 1, 2004

We elucidate the paraxial orbital angular momentum of entangled photon pairs generated by spontaneous parametric downconversion in different noncollinear geometries in which the entangled photons counterpropagate. We find, in particular, the orbital angular momentum of entangled pairs generated in transverse-emitting configurations, in which none of the known rules for selecting orbital angular momentum holds. © 2004 Optical Society of America

OCIS codes: 270.5290, 190.4410.

Spontaneous parametric downconversion (SPDC) is a reliable source of entangled photons.[1] The two-photon state it generates can be entangled, e.g., in polarization, spin angular momentum,[2] or frequency.[3] It can also be entangled in paraxial orbital angular momentum (OAM).[4] The corresponding multidimensional entangled states, or qudits, provide higher dimensional alphabets,[5] thus enhancing the potential of quantum techniques. The entangled two-photon state can be engineered by appropriate tailoring of the spatial characteristics of the pump beam,[6] as well as by use of transverse engineering of quasi-phase-matched geometries.[7]

To date, most investigations addressed SPDC in nearly collinear phase-matching geometries, in which the pump, the signal, and the idler photons propagate almost along the same direction. However, noncollinear geometries introduce a variety of new features. In particular, in noncollinear geometries both the spin angular momentum[8] and the OAM[9] of the entangled photons strongly depend on the propagation direction of the photons. In the classical domain, optical second-harmonic generation from two counterpropagating guide modes in a waveguide in a direction perpendicular to the surface of the waveguide was demonstrated,[10] backward second-harmonic generation was observed,[11] and the generation of tunable narrowband terahertz radiation was reported.[12] In the quantum domain it was shown that, when the counterpropagating entangled photons are emitted in a thin waveguide[13] or a waveguide with periodic nonlinearity,[14] their spectral bandwidth drastically decreases. In this Letter we elucidate the OAM of entangled photon pairs generated in different geometric configurations in which the entangled photons counterpropagate with respect to each other or to the pump (Fig. 1). We also find the orbital angular momentum of entangled pairs generated in purely transverse-emitting configurations, in which the known selection rules for the spiral index of the mode functions of the generated photons[4] no longer hold.

We consider a nonlinear optical crystal, illuminated by a quasi-monochromatic laser pump beam propagating in the z direction (Fig. 1). The two-photon quantum state $|\Psi\rangle$ at the output of the nonlinear crystal can be described by an effective Hamiltonian $H_I(t)$ in the interaction picture, given by[15] $H_I = \epsilon_0 \int_V \mathrm{d}^3V \chi^{(2)} E_p^+ E_s^- E_i^- + \text{c.c.}$, where E_p^+ refers to the positive-frequency part of the pump electric field operator and $E_{s,i}^-$ refer to the negative-frequency part of the signal and idler electric field operators. The amplitude field profile of the paraxial pump beam, which is treated classically, writes $E_p(\mathbf{x}, z, t) = \int \mathrm{d}\mathbf{q}_p E_0(\mathbf{q}_p) \exp[ik_p z + i\mathbf{q}_p \cdot \mathbf{x} - i\omega_p^0 t] + \text{c.c.}$, where $\mathbf{x} = (x, y)$ is the position in the transverse plane, z is the propagation direction of the pump beam, $\mathbf{q}_p$ is the transverse momentum, ω_p^0 is the angular frequency of the pump beam, $k_p(\mathbf{q}_p) = [(\omega_p^0 n_p/c)^2 - |\mathbf{q}_p|^2]^{1/2}$ is the longitudinal wave number inside the crystal, n_p is the refractive index at the pump wavelength,

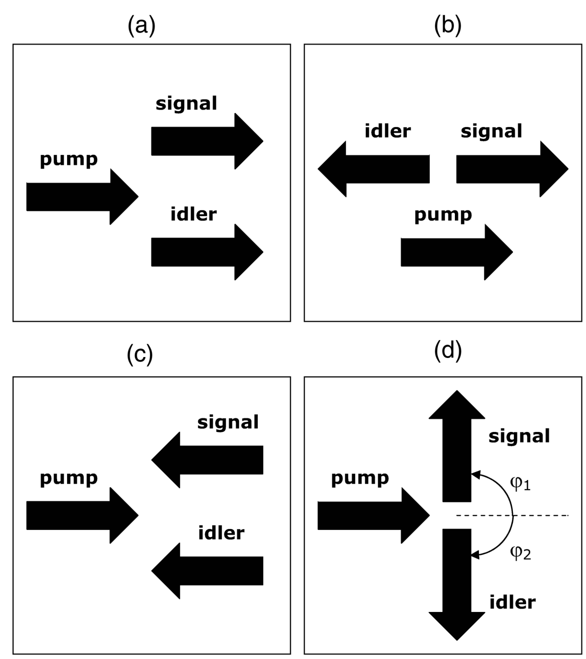

Fig. 1. Several noncollinear geometric configurations for SPDC. In (a) we show the usual collinear configurations for the sake of comparison. In (d) we show the angles φ_1 and φ_2.

0146-9592/04/161939-03$15.00/0

and $E_0(\mathbf{q}_p)$ is the field profile of the pump beam in momentum space. To devise the spatial structure of the generated two-photon state, we define $x_{1,2} = x$, $y_{1,2} = y \cos \varphi_{1,2} + z \sin \varphi_{1,2}$ and $z_{1,2} = z \cos \varphi_{1,2} - y \sin \varphi_{1,2}$, where $\varphi_{1,2}$ are the angles formed by the direction of propagation of the pump beam (z) and the direction of propagation of the signal (z_1) and idler photons (z_2). Electric field amplitude operator corresponding to the signal photon E_s^- can be written as

$$E_s^-(\mathbf{x}, z, t) \propto \int \mathrm{d}\omega_s \mathrm{d}\mathbf{p} \exp(-i\mathbf{p} \cdot \mathbf{x}_1 - ik_s z_1 + i\omega_s t) \times a_s^+(\omega_s, \mathbf{p}), \quad (1)$$

where $\mathbf{x}_1 = (x_1, y_1)$, $\mathbf{p} = (p_x, p_y)$ is the transverse momentum of the signal photon, $k_s(\mathbf{p}) = [(\omega_s n_s/c)^2 - |\mathbf{p}|^2]^{1/2}$ is the longitudinal wave number, a_s^+ is the creation operator, and n_s is the refractive index inside the nonlinear crystal at the signal wavelength. The situation is similar for the idler photon. In the first-order perturbation theory the quantum state of the two-photon state can be written as[16] $|\Psi\rangle = \int \mathrm{d}\omega_s \mathrm{d}\omega_i \mathrm{d}\mathbf{p}\mathrm{d}\mathbf{q} \Phi(\omega_s, \omega_i, \mathbf{p}, \mathbf{q}) \times a_s^\dagger(\omega_s, \mathbf{p}) a_i^\dagger(\omega_i, \mathbf{q}) |0, 0\rangle$, with $\Phi(\omega_s, \omega_i, \mathbf{p}, \mathbf{q}) = E_0(p_x + q_x, \Delta_0) \mathrm{sinc}(\Delta_k L/2) \exp(-i\Delta_k L/2)$, where $\Delta_k = k_p - k_s \cos \varphi_1 - k_i \cos \varphi_2 - p_y \sin \varphi_1 - q_y \sin \varphi_2 - 2\pi/\Lambda$ comes from the phase-matching condition in the z direction, $\Delta_0 = p_y \cos \varphi_1 + q_y \cos \varphi_2 - k_s \sin \varphi_1 - k_i \sin \varphi_2$, and $k_p = [(\omega_p^0 n_p/c)^2 - (p_x + q_x)^2 - \Delta_0^2]^{1/2}$. The signal and idler photons are assumed to be monochromatic, with $\omega_p^0 = \omega_s^0 + \omega_i^0$. To fulfill the phase-matching conditions, one should make use of quasi-phase matching. For degenerate SPDC ($\omega_s^0 = \omega_i^0$), period Λ is given by $\Lambda = \lambda_p^0/n_p$, where λ_p^0 is the wavelength in vacuum of the pump beam. The periodic modulation of the nonlinearity on such a small scale can be obtained with domain structures made of properly engineered asymmetric quantum wells[17,18] or by choosing grating periods such that higher-order quasi-phase matching can be achieved.

The spatial shape of the pump beam can be written as $E_0(\mathbf{q}_p) \propto (\rho_p/w_0)^{|l_0|} \exp(-\rho_p^2 w_0^2/4) \exp(il_0\varphi_p)$, where ρ_p and φ_p are the modulus and phase, respectively, of wave vector $\mathbf{q}_p$ and w_0 is the beam width. This shape corresponds to an optical vortex with an OAM per photon[19] equal to $l_0\hbar$. Most features of the configuration considered in this Letter can be revealed by analysis of the spatial shape of the signal photon after the idler photon is projected in one specific mode. We assume that the idler photon is projected into a Gaussian mode detector, through an appropriate lens system, followed by a monomode optical fiber and photodetector. The spatial mode function Φ_s can be written as $\Phi_s(\mathbf{p}) = \int \mathrm{d}\mathbf{q} \Phi(\mathbf{p}, \mathbf{q}) \exp(-|\mathbf{q}|^2 w_1^2/4)$, where w_1 is the width of the Gaussian mode. The spatial function Φ_s can be expressed by a mode decomposition into spiral harmonics,[5] i.e., $\Phi_s = \sum_{l_1} a_{l_1}(\rho_k) \exp(il_1\varphi_k)$, with ρ_k and φ_k being the modulus and phase, respectively, of wave vector $\mathbf{p}$. The weight of the distribution is given by $C_{l_1} = \int_0^\infty \rho_k \mathrm{d}\rho_k |a_{l_1}(\rho_k)|^2$, with $a_{l_1}(\rho_k) = 1/\sqrt{2\pi} \times \int_0^{2\pi} \mathrm{d}\varphi_k \Phi(\rho_k, \varphi_k) \exp(-il_1\varphi_k)$ and $\int |\Phi_s(\mathbf{p})|^2 \mathrm{d}\mathbf{p} = 1$. Quantum states whose mode function is shaped as $\exp(il\varphi_k)$ are eigenstates of the OAM operator with eigenvalue $l\hbar$.

Figure 2 shows the spatial shape and mode decomposition of the mode function of the signal photon for some configurations depicted in Fig. 1, when the pump beam is a vortex beam with $l_0 = 1$. Note that the shape of the spatial mode function can be observed when the signal photon is sent through an appropriately designed 2-f optical system.[16] The mode decomposition for $\varphi_1 = \varphi_2 = 0°$ [Fig. 1(a)] shows a single peak at $l_1 = 1$. This case corresponds to the signal and idler photons propagating in the same direction as the pump beam (forward). For $\varphi_1 = \varphi_2 = 180°$ [Fig. 1(c)], which corresponds to backward propagation for the signal and idler photons, a single peak appears at $l_1 = -1$. Projection of the idler photon into a Gaussian mode implies $l_2 = 0$, where l_2 refers to the OAM of the idler photon. For configurations in which $\varphi_1, \varphi_2 = 0°$ or $180°$ [Figs. 1(a)–1(c)], the condition

$$l_0 = s_1 l_1 + s_2 l_2 \quad (2)$$

is fulfilled, where $s_{1,2} = \pm 1$ correspond to forward (backward) propagation of the corresponding photon. This generalizes the selection rule that applies in the collinear case.[4] For $\varphi_1 = -\varphi_2 = 90°$ [Fig. 1(d)] the mode decomposition contains several modes. Indeed, the weight of modes $l_1 = 1$ and $l_1 = -1$ is equal. There is no simple relationship among l_0, l_1, and l_2,

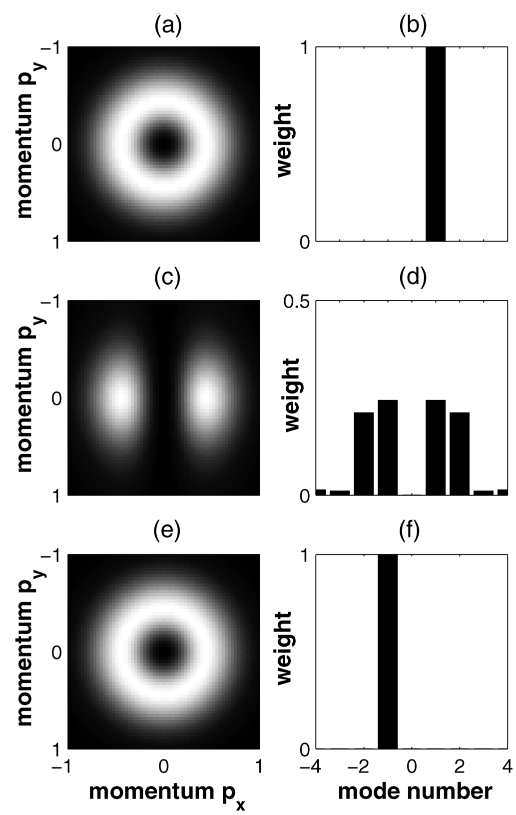

Fig. 2. Spatial shape and OAM decomposition of the mode function of the signal photon. (a), (b) $\varphi_1 = \varphi_2 = 0°$; (c), (d) $\varphi_1 = -\varphi_2 = 90°$; (e), (f) $\varphi_1 = \varphi_2 = 180°$. Parameters: $l_0 = 1$, $w_0 = 300$ μm, and $L = 1$ mm. The idler photon is projected into a Gaussian mode ($l_2 = 0$) with a mode width of $w_1 = 300$ μm. The momentum (p_x, p_y) is normalized to a beam width of $w = 100$ μm.

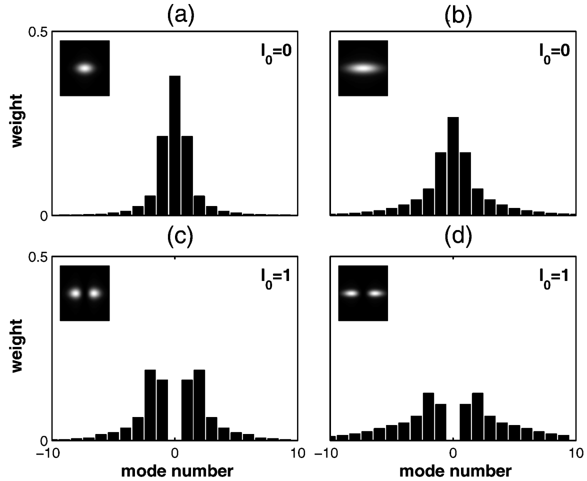

Fig. 3. OAM decomposition of the spatial mode function of the signal photon for $\varphi_1 = -\varphi_2 = 90°$. (a) $l_0 = 0$, $w_0 = 100\ \mu$m; (b) $l_0 = 0$, $w_0 = 50\ \mu$m; (c) $l_0 = 1$, $w_0 = 100\ \mu$m; (d) $l_0 = 1$, $w_0 = 50\ \mu$m. The crystal length is $L = 1$ mm. In all cases the idler photon is projected into a Gaussian mode ($l_2 = 0$) with a mode width of $w_1 = 300\ \mu$m. Insets, spatial shape of the mode function. The momentum (p_x, p_y) is normalized to a beam width of $w = 100\ \mu$m.

as is the case for configurations in which the photons copropagate or counterpropagate coaxially with the pump beam. Figure 3 shows the spatial mode function (inset) and the corresponding mode decomposition for different pump beam shapes for $\varphi_1 = -\varphi_2 = 90°$. The spatial shape of the mode function in the x_1 dimension depends on the shape of the pump beam in the corresponding dimension, whereas the shape in the y_1 dimension is tailored by the phase-matching condition in the longitudinal direction (z). As can be seen from Fig. 3, in all cases the spatial shape of the mode function in the x_1 dimension mimics the spatial shape of the pump beam in the corresponding dimension. This is in contrast with the collinear case, in which the ellipticity of Φ_s would not depend on the length of the nonlinear crystal.

Our predictions can be experimentally observed by use of a properly engineered higher-order quasi-phase-matching grating.[11] The resulting effective nonlinear coefficient at pump wavelengths of frequency-doubled Ti:sapphire lasers amounts to values similar to those of the nonlinear crystals commonly used in SPDC, such as critically phase-matched β-barium borate.

In conclusion, we have shown that the paraxial OAM of entangled photon pairs generated in noncollinear geometries in which the entangled photons counterpropagate exhibits new features in comparison with those known for collinear geometries. We generalized the selection rule connecting the OAM of the pump and the downconverted photons, known for copropagating geometries, to different counterpropagating settings in which the pump and the generated entangled photons are still coaxial. In noncoaxial, transverse-emitting geometries in which the known rules do not hold, we revealed that the OAM of the entangled photons is dictated by the geometric ellipticity of the generated spatial two-photon mode function. Importantly, such ellipticity is mediated by the shape of the pump beam and by the length of the nonlinear crystal, which is in sharp contrast with collinear phase matching.

This work was supported by the Generalitat de Catalunya and by the Spanish Government through grant BFM2002-2861. J. P. Torres's e-mail address is jperez@tsc.upc.es.

References

1. D. Bouwmeester, A. Ekert, and A. Zeilinger, eds., *The Physics of Quantum Information* (Springer-Verlag, Berlin, 2000).
2. P. G. Kwiat, K. Mattle, H. Weinfurter, A. Zeilinger, A. V. Sergienko, and Y. Shih, Phys. Rev. Lett. **75,** 4337 (1995).
3. C. K. Law, I. A. Walmsley, and J. E. Eberly, Phys. Rev. Lett. **84,** 5304 (2000).
4. A. Mair, A. Vaziri, G. Weihs, and A. Zeilinger, Nature **412,** 313 (2001).
5. G. Molina-Terriza, J. P. Torres, and L. Torner, Phys. Rev. Lett. **88,** 013601 (2002).
6. J. P. Torres, Y. Deyanova, L. Torner, and G. Molina-Terriza, Phys. Rev. A **67,** 052313 (2003).
7. J. P. Torres, A. Alexandrescu, S. Carrasco, and L. Torner, Opt. Lett. **29,** 376 (2004).
8. A. Migdall, J. Opt. Soc. Am. B **14,** 1093 (1997).
9. G. Molina-Terriza, J. P. Torres, and L. Torner, Opt. Commun. **228,** 155 (2003).
10. R. Normadin and G. I. Stegeman, Opt. Lett. **4,** 58 (1979).
11. J. U. Kang, Y. J. Ding, W. K. Burns, and J. S. Melinger, Opt. Lett. **22,** 862 (1997).
12. C. Weiss, G. Torosyan, Y. Avetisyan, and R. Beigang, Opt. Lett. **26,** 563 (2001).
13. A. De Rossi and V. Berger, Phys. Rev. Lett. **88,** 043901 (2002).
14. M. C. Booth, M. Atature, G. Di Giuseppe, B. E. A. Saleh, A. V. Sergienko, and M. C. Teich, Phys. Rev. A **66,** 023815 (2002).
15. D. N. Klyshko, Sov. Phys. JETP **28,** 522 (1969).
16. B. E. A. Saleh, A. F. Abouraddy, A. V. Sergienko, and M. C. Teich, Phys. Rev. A **62,** 043816 (2000).
17. J. B. Khurgin, Phys. Rev. B **38,** 4056 (1988).
18. S. Janz, F. Chatenoud, and R. Normandin, Opt. Lett. **19,** 622 (1994).
19. L. Allen, M. J. Padgett, and M. Babiker, in *Progress in Optics*, E. Wolf, ed. (Elsevier, New York, 1999), Vol. 39, pp. 291–372.